ELSEVIER

Journal of Alloys and Compounds 248 (1997) 59–65

Journal of ALLOYS AND COMPOUNDS

The effect of layer thickness and composition on the kinetics of solid state reactions in the niobium–selenium system studied using superlattice reactants

Masafumi Fukuto[a], Jeff Anderson[a], Marc D. Hornbostel[a], David C. Johnson[a,*], Hsiumin Huang[b], Stephen D. Kevan[b]

[a]*Department of Chemistry and Materials Science Institute, Eugene, OR 97403, USA*
[b]*Department of Physics and Materials Science Institute, Eugene, OR 97403, USA*

Received 28 May 1996; revised 3 August 1996

Abstract

The ability to form an amorphous reaction intermediate by the low temperature interdiffusion of a modulated elemental reactant is shown to be a function of the overall composition as well as elemental layer thicknesses in the niobium–selenium system. For niobium-rich reactants, an amorphous reaction intermediate was observed to form upon low temperature annealing of reactants with modulation thicknesses less than 60 Å. Further annealing of the amorphous intermediates led to the crystallization of Nb_2Se, Nb_5Se_4 or Nb_3Se_4 depending upon the overall composition of the amorphous intermediate. Modulated elemental reactants with overall compositions containing more than two-thirds selenium were found to heterogeneously nucleate $NbSe_2$ at the reacting interfaces. The formation of the thermodynamically expected compounds Nb_2Se_3, $NbSe_3$, and Nb_2Se_9 at their respective compositions required extended high temperature annealing to react the dichalcogenide with the remaining elemental reactants. A striking difference between the evolution of the low angle diffraction patterns in these two composition regimes suggests the differences in the reaction kinetics result from a composition dependence of the diffusion coefficients.

Keywords: Niobium–selenium system; Kinetics; Solid state reactions; Superlattice reactants

1. Introduction

The high reaction temperatures and long reaction times typically used in classical solid state chemistry result in thermodynamically stable products. Since the vast majority of all known solid state compounds have been produced using similar reaction conditions, there has been little emphasis placed upon the kinetics or mechanisms of solid state reactions [1,2]. A typical synthesis involves simply mixing elements at a specific atomic ratio and heating until a single phase product is formed. The sequence of intermediate phases, as well as the kinetics of each transformation, are not determined and are completely uncontrolled. In binary systems, it is possible to systematically study reactivity between two elements by forming a diffusion couple. This consists of a bulk piece of each element joined at a well-defined interface. These have been used to study binary phase diagrams because, after extended annealing, all stable compounds will form [3]. However, even in these simple systems, there was very little work on the sequence of phase formation or the kinetics of reactions until the late 1970s.

The interest in the kinetics of solid state reactions resulted from the semiconductor community's desire to control the thickness and purity of thin metal silicide contacts formed during device manufacturing processes. It was soon well established experimentally that the evolution of thin-film planar binary diffusion couples proceeds through a sequence of binary compounds [4–7]. In the transition metal silicides, one compound was observed to form reproducibly and grow between the reactants irrespective of the relative amounts of the metal or silicon reactant. If the film was thin enough, the growth of the initial compound was found to exhaust the supply of one of the reactants before a second compound was formed.

*Corresponding author.

0925-8388/97/$17.00
PII S0925-8388(96)02650-3

Thus a sequential evolution of interfacial compounds was observed [8].

Several empirical rules were formulated to predict the phase which formed first using information in equilibrium phase diagrams. The first phase rule of Walser and Bené, which states "The first compound nucleated in planer reaction couples is the most stable congruently melting compound adjacent to the lowest temperature eutectic on the bulk equilibrium phase diagram," is typical [9]. It is based on the idea of an amorphous material initially forming between the reactants with a composition near that of the lowest temperature eutectic — the most stable liquid in the equilibrium phase diagram. It is then assumed that the easiest compound to nucleate will be the most stable compound closest in composition to the glassy, interfacial phase. Similar empirical rules have been developed to explain the sequence of phase formation in metal–metal and other binary diffusion couples [10–12].

In the bulk diffusion couples and the thin film diffusion couples described above, the initial compound forms at the interface and it does not depend upon the overall composition of the diffusion couple. In the mid-1980s, it was discovered that if the thickness of the reacting layers was decreased it was possible to avoid interfacial nucleation and form an amorphous material [13–16]. Various investigators have found there are critical layer thicknesses for the transition between this ultra-thin and thin film behavior [15,17,18]. It has been proposed that this critical thickness depends upon the competition between interdiffusion and nucleation. This is based upon the idea that it takes less energy to nucleate at an interface than in the bulk. If the interface moves past the organizing nucleus before it reaches the critical size, crystallization will not occur. Since movement of the interfaces slows down as the diffusion lengths increase, eventually a nucleus will grow large enough and nucleate crystallization while still in the interface [19]. The thickness of the elemental layers required for interfacial nucleation to occur is referred to as the critical layer thickness.

This paper addresses the transition region between the ultra-thin film and thin film regimes in the niobium–selenium binary system, asking whether the critical thickness in a system is dependent on composition and whether the first phase formed at an interface depends upon the overall composition when one is near this critical length scale. The niobium–selenium system was chosen for this study because the phase diagram contains seven different compounds: Nb_2Se, Nb_5Se_4, Nb_3Se_4, Nb_2Se_3, $NbSe_2$, $NbSe_3$, and Nb_2Se_9. Each of these compounds has a narrow composition range, and all differ significantly in structure [20]. This permits the study of the extent to which the composition and the layer thickness of the multilayer control which of the many possible compounds crystallizes. In particular, the compound $NbSe_2$ is difficult to avoid in conventional high temperature synthesis, presumably because it is the initial compound to nucleate at the reacting interfaces.

2. Experimental section

2.1. Synthesis of samples

Samples were made in a custom-built ultra-high vacuum chamber with independently controlled sources. Above each of the sources are computer-controlled shutters to allow precise control of elemental layer thicknesses [21]. Niobium was deposited by an electron-beam gun that was controlled via a Leybold-Inficon XTC quartz crystal thickness monitor. Niobium was deposited at 0.5 Å s^{-1} and the niobium thickness desired was obtained by opening the shutter for a constant time period for each layer. Selenium was deposited using a Knudsen cell maintained at a constant temperature by an Omega CN-9000 temperature-controller. The rate of selenium deposition was monitored on a quartz crystal thickness monitor and the temperature of the cell was chosen to maintain a selenium deposition rate of approximately 1.0 Å s^{-1}. Desired selenium layer thicknesses were obtained by integrating the thickness measured by the crystal monitor and closing the shutter after accumulating the desired Se thickness.

The procedure for making these samples is to degas each of the sources to be used, then to start each source depositing. Once each of the source's deposition rate has stabilized, the samples are manufactured a set at a time. This is done by moving a sample set above a source, opening the shutter, depositing the desired amount, closing the shutter and moving onto the next source. Each sample set consists of an X-ray and a differential scanning calorimetry (DSC) silicon substrate. The silicon substrates used for X-ray studies are polished to ±3 Å r.m.s. The substrates used for DSC studies are silicon wafers coated with poly(methyl methacrylate) (PMMA).

2.2. Grazing- and high-angle X-ray diffraction

X-ray data were collected on a Scintag 2000 θ–θ diffractometer which had been modified to allow the sample height to be reproducibly adjusted by 0.0002 in. Alignment of the diffractometer was confirmed by checking that the rocking curve maxima due to specular reflection at several angles occurred when the incident and exit angles were equal. Grazing-angle X-ray diffraction data were used to confirm the layered structure of the starting superlattice and to determine the layer spacing. High-angle diffraction data were used to determine whether a film contained crystalline elements or compounds. During the interdiffusion study, samples were annealed in a drybox with a nitrogen atmosphere containing less than 0.5 ppm oxygen.

2.3. DSC

The heat produced and absorbed by diffusion, compound nucleation and growth in the Nb–Se superlattices

was measured using a Du Pont TA9000 DSC module. Approximately 2 mg of sample free of the substrate was used in this experiment. The sample was obtained by first coating a 4 in silicon wafer with PMMA. This was done using a 3% solution of PMMA in chlorobenzene and a spincoater rotating at 1000 rev min^{-1}. The desired Nb–Se layers were then deposited on the substrate. A piece of the deposited substrate was then placed in acetone, which dissolved the PMMA and left the sample floating free. The sample, which typically broke into small pieces, was gathered by sedimentation into an aluminum DSC pan. Excess acetone was dried off under vacuum, and then the pan was crimped closed.

The sample was placed in the DSC with an empty aluminum pan as a reference. The sample was heated to 600 °C at a rate of 10 °C min^{-1} under flowing nitrogen. The sample was cooled and reheated to 600 °C twice more to obtain baselines of the reversible changes in the sample. A comparison of the two baselines gives a measure of the repeatability of the experiment. The net heat absorbed or released from the multilayer samples during the irreversible changes that occurred during the initial heating was obtained from the difference between the first and the subsequent runs.

2.4. Thermogravimetric analysis (TGA)

TGA was used to determine the actual stoichiometry of the original layered sample. A sample was floated off of the PMMA-coated substrate and then dried. The sample was then weighed in a platinum pan on a microbalance. The sample was then heated to 700 °C in flowing air and then held at this temperature for 2 h. The weight change recorded was the difference between mass loss due to the evaporation of Se and the weight gain resulting from the oxidation of the niobium forming Nb_2O_5, as confirmed by X-ray diffraction.

3. Results and discussion

Table 1 contains a summary of the 15 samples prepared during this investigation as we varied composition and layer thickness. The range of layer thicknesses in these samples was limited to elemental layer thicknesses greater than 5 Å by our ability to detect diffraction maxima in the low angle diffraction patterns of the superlattices. In samples with thick layers, an endotherm corresponding to selenium melting was observed. Since we were interested in solid phase reactions, this provided an upper limit of 50 Å for the selenium layer thickness. For all of the samples studied, the measured thicknesses of the repeating bilayer units obtained by indexing the low angle diffraction patterns were within several angstroms of the intended thicknesses, and the measured compositions were proportional to the ratio of the intended niobium thicknesses divided by the selenium thicknesses to within the errors

Table 1
A summary of intended elemental layer thicknesses, measured thicknesses of the repeating units and measured composition of the samples from TGA for the Nb–Se multilayer samples prepared

Sample	Intended Nb thickness (Å)	Intended Se thickness (Å)	Measured thickness (Å)	Measured Nb/Se ratio
33	8.4	36.2	44	0.33
34	8.4	31.0	39	0.36
31	16.8	25.8	41	0.55
50	7.6	6.7	16	0.55
86	16.4	37.2	47	0.67
co11	10.0	90.0	96	0.69
67	9.6	6.7	15	0.86
70	19.0	24.8	47	0.88
56	21.0	15.5	40	1.14
57	15.4	9.8	25	1.14
37	11.7	7.8	18	1.23
55	27.7	22.7	52	1.32
58	48.9	48.0	95	1.51
61	134.0	96.1	204	1.39
77	19.2	5.1	24	2.10
83				3.02

expected from the reproducibility of the deposition monitors. The largest deviations between the intended and measured total thicknesses occur for samples with large selenium layer thicknesses, where the measured thickness is significantly lower than the intended values. We think this deviation results from a change in the probability of selenium sticking to the surface as the surface composition changes. The probability of a selenium atom sticking to a niobium surface is higher than the probability of a selenium atom sticking to a selenium surface.

The evolution of these niobium–selenium multilayer reactants as a function of increasing temperature was followed using DSC combined with both low and high angle X-ray diffraction. The DSC measurements provide a fast overview of the irreversible exothermic and endothermic reactions which occur during the initial heating of the samples. The diffraction measurements allow us to correlate interdiffusion and crystallization with transitions observed in the DSC. The observed reaction kinetics divide the samples into two distinct groups based upon the composition of the multilayer reactant.

Multilayer reactants on the niobium-rich side of the phase diagram were observed to interdiffuse forming an amorphous intermediate for total layer thicknesses less than 60 Å. Increasing the temperature of the amorphous intermediates resulted in the formation of known crystalline compounds, with the overall composition of the amorphous intermediate determining which compound nucleated. DSC data collected on the two most metal-rich samples, samples A-1 and A-2, contain a broad exotherm between 350 and 550 °C. X-ray diffraction after this exotherm indicates that the samples are still amorphous with respect to X-ray diffraction. After annealing at higher temperature, diffraction data show that the sample contains Nb_2Se. DSC of samples C-1–C-4 show a broad exotherm

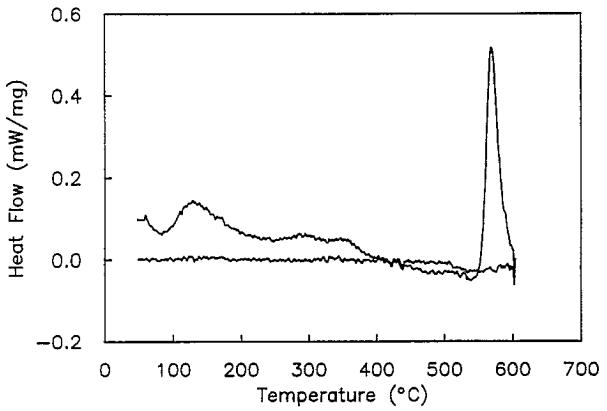

Fig. 1. DSC data collected on sample C-1 at a scanning rate of 10 °C min^{-1}.

between 100 and 400 °C followed by a sharp exotherm at 570 °C, as shown in Fig. 1. Low angle X-ray diffraction data collected as a function of annealing temperature indicate that the broad exotherm results from interdiffusion of the elemental layers. High angle X-ray diffraction data indicated that the sample formed an amorphous intermediate during the interdiffusion of the layers. The sample crystallized during the sharp exotherm, forming Nb_5Se_4, as shown in Fig. 2. DSC data collected on samples D-1 and D-2 contained a broad exotherm between 100 and 200 °C. Low angle diffraction data collected as a function of temperature indicate that the layers interdiffuse during this exotherm. High angle diffraction data indicate that the samples remain amorphous on repeated temperature cycling to 550 °C but crystallize, forming Nb_3Se_4, upon heating to 600 °C, as shown in Fig. 3.

The two thicker metal-rich samples studied, samples B-1 and B-2, formed microcrystalline Nb during low temperature annealing. Higher temperature annealing resulted in the formation of Nb_5Se_4. The particle sizes, determined from the X-ray diffraction line widths and the Scherrer

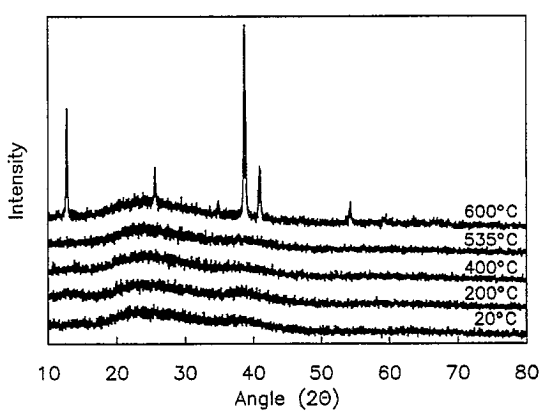

Fig. 2. X-ray diffraction scans collected on a second portion of sample C-1 after annealing at the temperatures indicated. The diffraction pattern collected after annealing at 600 °C matches that given in the JCPDS diffraction file for Nb_5Se_4.

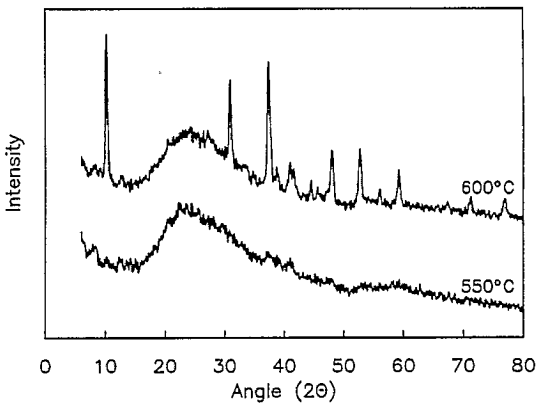

Fig. 3. X-ray diffraction scans collected on a portion of sample D-2 after annealing at the temperatures indicated. The diffraction pattern collected after annealing at 600 °C matches that given in the JCPDS diffraction file for Nb_3Se_4.

equation, scale with the layer thicknesses of the initial reactant, suggesting that interfacial nucleation occurs at the microcrystalline niobium–amorphous-niobium–selenium alloy interface. Unfortunately, the solid state reaction of more selenium-rich samples was prevented by the observation of an endotherm in the DSC corresponding to the melting of the thick selenium layers in these samples.

In contrast to the niobium-rich samples discussed above, the multilayer reactants with overall compositions containing more than two-thirds selenium (samples E-1 through E-6) were found to heterogeneously nucleate $NbSe_2$ at the interfaces regardless of initial elemental layer thicknesses or composition within this regime. Fig. 4 contains DSC data of a representative sample (E-5) exhibiting the broad low temperature exotherm characteristic of samples in this composition range. Low angle diffraction data collected as a function of temperature, shown in Fig. 5, indicate that the sample is still compositionally modulated during this low temperature exotherm. The high angle diffraction data, shown in Fig. 6, indicate that $NbSe_2$ has formed while the sample is still

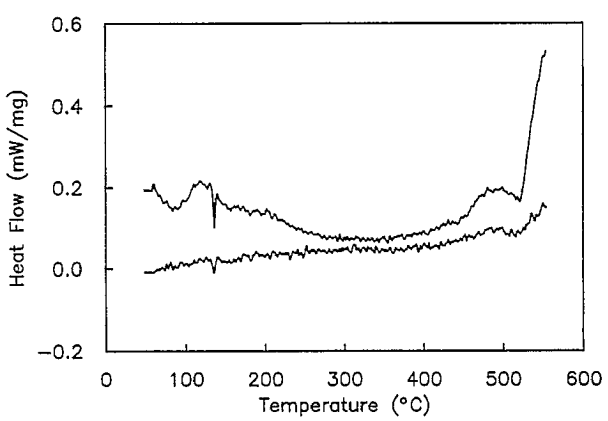

Fig. 4. DSC data collected on sample E-5 at a scanning rate of 10 °C min^{-1}

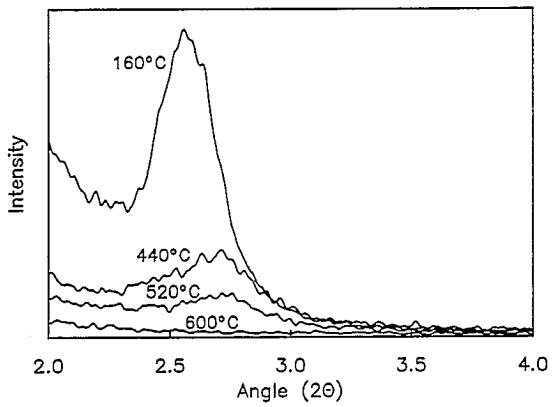

Fig. 5. Low angle diffraction data collected on a portion of sample E-5 after annealing at the temperatures indicated. The diffraction maxima at approximately 2.5° indicate that the sample is still compositionally modulated after annealing at 520 °C.

compositionally modulated, with small crystallites present by 160 °C. The crystalline $NbSe_2$ product was oriented with its crystallographic *c*-axis parallel with the layering direction. The diffraction and DSC data suggested that the $NbSe_2$ product nucleates at and grows along each reacting planar interface.

As we changed the ratio of niobium to selenium layer thicknesses, and therefore the overall composition of the film, we observed the formation of $NbSe_2$ over a wide composition range. This suggests that it is a kinetic product, since the phase diagram states that other solid state compounds are thermodynamically more stable than a mix of the elements and $NbSe_2$ at these compositions. Extended annealing eventually leads to their formation. Further evidence for interfacial nucleation comes from the formation of Nb_5Se_4 upon continued annealing of sample E-5, rather than the thermodynamically expected Nb_2Se_3. Since the sample is still layered while Nb_5Se_4 is formed, we suspect that Nb_5Se_4 heterogeneously nucleates at the niobium–$NbSe_2$ interface. Presumably, Nb_5Se_4 forms as a result of a lower nucleation barrier, as indicated by its more facile nucleation observed as we studied the evolution of the more niobium-rich samples.

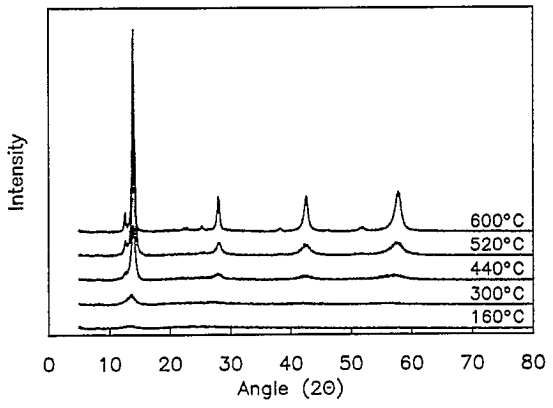

Fig. 6. High angle X-ray diffraction scans collected on a sample E-5 after annealing at the temperatures indicated. The position of the diffraction maxima coincide with that expected for the 00*l* peaks of $NbSe_2$.

The reaction kinetics observed in the samples studied can be summarized in a kinetic analog of a phase diagram, plotting initial crystalline compound observed on a graph of the layer thicknesses of the reacting superlattices vs. their average composition (Fig. 7). This graph highlights the interplay between initial reaction kinetics, overall composition and layer thickness. Samples with total layer thickness less than 60 Å and niobium composition greater than 45% interdiffuse to form an amorphous intermediate. Samples with niobium composition less than 45% heterogeneously nucleate $NbSe_2$. This preferential nucleation of $NbSe_2$ obviously depends strongly on the size and complexity of the critical nucleus which has to form for each of the phases in this composition region. If the size and complexity of the critical nucleus is correlated with the size and complexity of the crystallographic unit cell, this would explain the preferential nucleation of $NbSe_2$. $NbSe_2$ has a very simple structure compared with the structure of the compounds Nb_2Se_9, $NbSe_3$ and Nb_2Se_3. Since the dependence of the initial reaction kinetics on composition and layer thickness may also result from differences in the development of composition gradients at the interface, we studied the interdiffusion of two multilayer films using low angle diffraction.

Two additional samples were prepared for the interdiffusion experiment on polished silicon wafers, a niobium-rich multilayer with 20 Å of niobium and 25 Å of selenium and a selenium-rich multilayer with 20 Å of niobium and 62 Å of selenium. The low and high angle diffraction patterns were collected as a function of annealing temperature. The low angle diffraction patterns are shown in Fig. 8 Fig. 9.

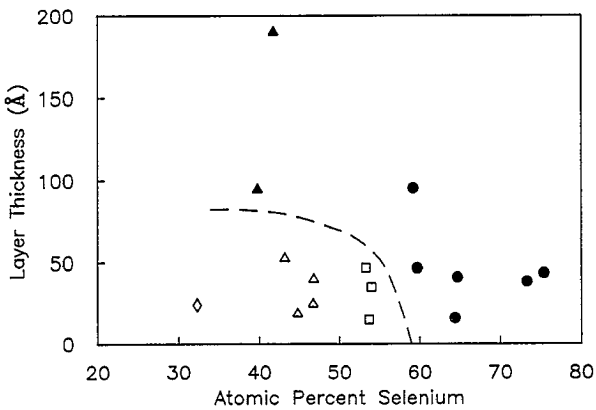

Fig. 7. The reaction behavior of the samples studied summarized in a kinetic analog of a phase diagram, plotting initial crystalline compound observed on a graph of the layer thicknesses of the reacting superlattices vs. their average composition. Open symbols indicate that an amorphous intermediate was formed; filled circles indicate that compound formation occurred while the sample was still compositionally modulated. Initial formation of $NbSe_2$ is indicated by circles, Nb_3Se_4 by squares, Nb_5Se_4 by triangles, and Nb_2Se by diamonds.

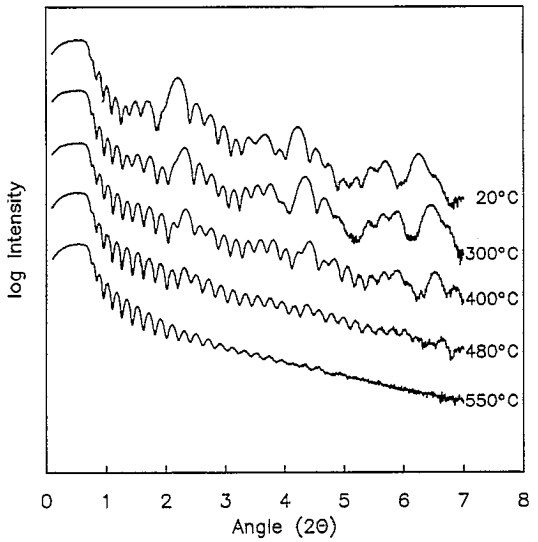

Fig. 8. Evolution of low angle diffraction pattern of a niobium-rich sample as a function of annealing temperature. The more intense and broad diffraction maxima are a consequence of the compositional modulation in the sample, while the higher frequency diffraction maxima are a consequence of interference between X-rays scattered from the top and bottom of the multilayer sample.

Both the high and low angle diffraction data of the interdiffusion experiment samples are consistent with the results of the free-standing samples studied using DSC and X-ray diffraction. There is a striking difference between the evolution of the low angle diffraction patterns of the two samples with annealing temperature. The selenium-rich sample interdiffuses rapidly and heterogeneously

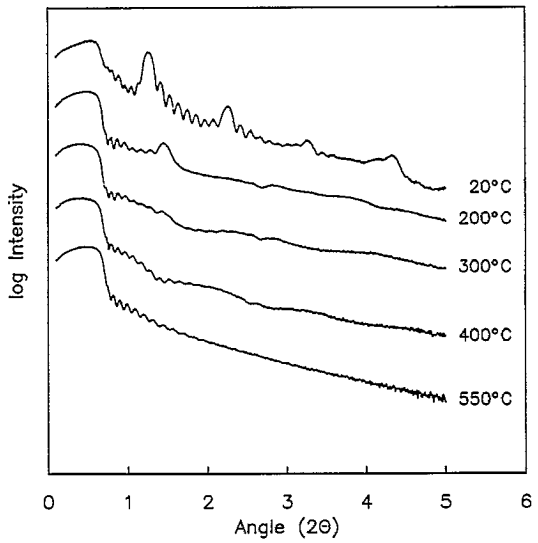

Fig. 9. Evolution of low angle diffraction pattern of a selenium-rich sample as a function of annealing temperature. The more intense and broad diffraction maxima are a consequence of the compositional modulation in the sample, while the higher frequency diffraction maxima are a consequence of interference between X-rays scattered from the top and bottom of the multilayer sample.

nucleates $NbSe_2$ at the interfaces by 300 °C. The low angle diffraction maxima of the niobium-rich sample have completely disappeared by 480 °C, and the high angle diffraction data show that the sample remains X-ray amorphous up to 550 °C. After annealing at 550 °C the diffraction pattern contains small diffraction maxima at 16, 38 and 41° indicating that Nb_5Se_4 has nucleated.

The selenium-rich sample interdiffused at a substantially faster rate. Only the first-order low angle diffraction maxima were visible after annealing at 200 °C for 1 h, even though the period of the modulation was almost twice that of the niobium-rich sample. By comparison, the niobium-rich sample which was annealed in the same furnace at the same time showed only minor changes in the low angle diffraction pattern. Based upon the change in the diffraction patterns after 1 h annealing at 200 °C, the interdiffusion rate in the selenium-rich sample is at least an order of magnitude faster than that found in the niobium-rich sample. This is consistent with a composition-dependent interdiffusion coefficient, where interdiffusion is faster in selenium-rich regions than niobium-rich regions.

The composition dependence of the interdiffusion coefficient also provides a clue to the observed reaction kinetics, since nucleation is very sensitive to the developing concentration gradients at the reacting interfaces. In selenium-rich samples, the fast interdiffusion rates quickly lead to a broad composition plateau which spans the composition range of $NbSe_2$, facilitating its heterogeneous nucleation. In niobium-rich samples, the initial interdiffusion increases the niobium concentration in the selenium regions of the multilayer but the samples still remain compositionally modulated. We suspect that $NbSe_2$ does not heterogeneously nucleate in these samples because the interfacial region contains only a small spatial area of this composition. This hypothesis can be verified by studying the time-dependent composition profile as a function of overall composition. Based on our studies, and by analogy to what is observed in silicide systems [18], we predict that selenium-rich samples form an amorphous concentration plateau which has a composition near 1:2 Nb:Se. We expect niobium diselenide nucleates at the interfaces between this composition plateau and the remaining elemental reactants.

4. Summary

The results presented demonstrate the importance of overall composition and layer thicknesses on subsequent reaction kinetics of modulated elemental reactants. In the metal-rich region investigated we observed the formation of an amorphous reaction intermediate. The crystalline product which nucleates from this intermediate was found to be determined by the average composition, with either Nb_2Se, Nb_5Se_4 or Nb_3Se_4 forming. Multilayered elemental reactants which were more selenium-rich were found to nucleate $NbSe_2$ heterogeneously at the internal interfaces.

This heterogeneous nucleation prevented the formation of the thermodynamically expected compounds Nb_2Se_3, $NbSe_3$, and Nb_2Se_9 at their respective compositions. We believe that this results from the formation of a broad composition plateau at the reacting interfaces which spans the composition range of $NbSe_2$, facilitating its interfacial nucleation.

Acknowledgments

This work was supported by the National Science Foundation (DMR-9213352 and DMR-9308854). Additional support by the Office of Naval Research (N0014-93-1-0205) and the University of Oregon is gratefully acknowledged.

References

[1] F.J. DiSalvo, *Science, 247* (1990) 649.
[2] A. Stein, S.W. Keller and T.E. Mallouk, *Science, 259* (1993) 1558.
[3] J.H. Brophy, R.M. Rose and J. Wulff, *Thermodynamics of Structure*, Vol. 2, Wiley, New York, 1964.
[4] G. Ottaviani, *Mater. Res. Soc. Symp. Proc., 25* (1984) 21.
[5] G. Ottaviani and C. Nobili, *Thin Solid Films, 163* (1988) 111.
[6] J.W. Mayer, J.M. Poate and K.-N. Tu, *Science, 190* (1975) 228.
[7] K.L. Holloway, Interfacial reactions in metal–silicon multilayers, *Ph.D. Thesis*, Stanford University, 1989.
[8] K.N. Tu and J.W. Mayer, in J.M. Poate, K.N. Tu and J.W. Mayer (eds.), *Thin Films—Interdiffusion and Reactions*, Wiley-Interscience, New York, 1978, Chapter 10.
[9] R.M. Walser and R.W. Bené, *Appl. Phys. Lett., 28* (1976) 624.
[10] R. Pretorius, *Mater. Res. Soc. Symp. Proc., 25* (1984) 15.
[11] E.G. Colgan and J.W. Mayer, *J. Mater. Res., 4* (1989) 815.
[12] R.W. Bené, *Appl. Phys. Lett., 41* (1982) 529.
[13] R.B. Schwarz, K.L. Wong and W.L. Johnson, *J. Non-Cryst. Solids, 61–62* (1984) 129.
[14] R.B. Schwarz and W.L. Johnson, *Phys. Rev. Lett., 51* (1983) 415.
[15] E.J. Cotts, W.J. Meng and W.L. Johnson, *Phys. Rev. Lett., 57* (1986) 2295.
[16] W.L. Johnson *Prog. Mater. Sci., 30* (1986) 81.
[17] L. Fister and D.C. Johnson, *J. Am. Chem. Soc., 114* (1992) 4639.
[18] K. Holloway and R. Sinclair, *J. Appl. Phys., 61* (1987) 1359.
[19] U. Gösele and K.N. Tu, *J. Appl. Phys., 66* (1989) 2619.
[20] T.B. Massalski, H. Okamoto, P.R. Subramanian and L. Kacprzak, *Binary Alloy Phase Diagrams*, Vol. 3, ASM International, 2nd edn., 1990, pp. 2664–2665.
[21] L. Fister, X.M. Li, T. Novet, J. McConnell and D.C. Johnson, *J. Vac. Sci. Technol. A, 11* (1993) 3014.